*Materials Transactions, JIM*, Vol. 36, No. 2 (1995), pp. 282 to 288

# Raman Spectra of Graphite and Diamond Mechanically Milled with Agate or Stainless Steel Ball-Mill

K. Niwase*, T. Tanaka**, Y. Kakimoto*,
K. N. Ishihara*** and P. H. Shingu***

*Hyogo University of Teacher Education, Yashiro-cho, Hyogo 673-14, Japan
**Department of Mechanical Engineering, Faculty of Engineering, Osaka Sangyo University, Daito, Osaka 574, Japan
***Department of Energy Science and Engineering, Kyoto University, Yoshida, Sakyo-ku, Kyoto 606-01, Japan

The reduction of crystalline size and amorphization of graphite and diamond during agate and stainless ball-milling are investigated by Raman spectroscopy. The ultimate crystalline size of graphite, estimated by the Raman intensity ratio, of 2.5 nm for the agate ball-mill is smaller than that of 3.5 nm for the stainless ball-mill, while the milling time to reach the ultimate size for the former is about 10 times larger than for the latter, indicating more stability of the nanocrystalline graphite. After reaching the ultimate crystalline size, a significant broadening of the Raman spectra, which indicates the completion of amorphization, is detected only for the stainless ball-milled graphite at ~500 h of milling. Also the increase rate of the Raman peakwidth for the stainless ball-milled graphite before amorphization is higher than that for the agate ball-milled graphite, indicating a larger introduction of disorder from the start of milling. Amorphization of diamond is also observed for the stainless ball-mill. The difference in the results between the agate and the stainless ball-mill is discussed in terms of the effect of impurity mixed from the milling apparatus on the stability of nanocrystalline carbon materials.

(Received October 24, 1994)

*Keywords*: *graphite, diamond, ball-milling, mechanical alloying, Raman spectroscopy, amorphous, surface enhanced Raman scattering*

## I. Introduction

Ball milling or mechanical alloying has been widely utilized to synthesize new materials such like amorphous alloy, metal-ceramic composites, and quasicrystalline phase, etc. More recently, ball milling has been used to produce nanocrystalline materials, which have unique atomic structure and promises interesting technological applications. Until now nanocrystalline metals with a grain size ranging from 5 to 22 nm have been obtained by ball milling for fcc, bcc and hcp[1]-[3] but crystal-amorphous phase (C-A) transition has not been reported for these elemental metals.

C-A transition by ball-milling as a pure element has been only found for silicon[4], which is also known as one of elements which amorphizes by high energy particle irradiation[5]. For C-A transition to proceed, the free energy of the crystal has to be raised above the free energy of the amorphous phase. The amorphization of Si by ball-milling is explained by a refinement of the grain size of the particle which leads to a destabilization of the diamond structure. UP to now, however it is not still clear how the nanocrystalline materials is destabilized by mechanical deformation.

Graphite is one of elements which amorphizes by electron[6] and ion irradiation[7], while diamond as an allotrope of graphite does not amorphize by electron irradiation[8] though it amorphizes by ion irradiation[9][10]. Recently, it has been shown that high concentration of vacancies in irradiated graphite can induce instability of graphite structure, leading to gradual transformation to the amorphous phase[11].

In this study, we aim to produce nanocrystalline graphite with two types of ball-mills, consisting of different media of agate and stainless steel, and to clarify the stability of nanocrystalline graphite in terms of crystalline size and chemical bonding with impurity mixed during milling. Also the structural change of diamond during stainless ball-mill is investigated.

## II. Experimental

Elemental powders of graphite (99.9%; average size, 5 $\mu$m) and industrial diamond made by General Electric Co. (average size, 110 $\mu$m) were used as starting material. Two types of milling apparatus were used, which are:

(i) Agate cylindrical vials mounted on a planetary ball-mill (P-7). The vial contains 7 agate balls each with a diameter of 15 mm. The mass of the sample was 1 g, and the weight ratio of sample to ball was 1:32.

(ii) A conventional ball-mill, of which the vial (1600 $cm^3$) and the ball (9.5 mm in diameter) are made of stainless steel. The mass of the sample was 40 g, and the weight ratio of sample to ball was 1:100.

For graphite, the above two types of milling were given in argon atmosphere. Two series of milling of 0~2000 h and 3000~5000 h were held for the type (ii). We refer to

the type (i) and the type (ii) as the agate ball-mill and the stainless ball-mill to distinguish the media of the two milling apparatuses, hereafter. For diamond, on the other hand, milling was given only the type (i), changing the vials and balls from agate to stainless steel: the mass of the diamond sample was 1 g, and the weight ratio of sample to ball was 1:96.

After different time periods, a small amount of sample was taken out in a glove-box filled with argon gas. The structural changes of graphite and diamond by the ball-millings were investigated by means of Raman spectroscopy. Raman scattering measurements were performed about 3 times for each sample at RT using a back-scattering geometry with the 514.5 nm line of an argon laser. Scattered light from the specimen was dispersed with a triple polychrometer (SPEX 1877) and acquired in a multichannel detector (Princeton Instruments H-SIDA700).

## III. Results

Figures 1(a) and (b) compare the variation in Raman spectra for graphite powders milled with the agate and the stainless ball-mills as a function of milling time, respectively. The Raman spectrum of the virgin graphite is shown at the bottom in the figure, which has a very small defect peak at 1355 $cm^{-1}$ (D-peak) in addition to an intense original graphite peak at $\sim$1580 $cm^{-1}$ (G-peak). For the agate ball-mill, the D-peak is seen to gradually increase in intensity against the G-peak but the changes in their peakwidths are not significant up to 1750 h of milling. For the stainless ball-mill, on the other hand, the intensity ratio of the two peaks ($I_{1355}/I_{1580}$) gradually increases up to 50 h and then both the peakwidths of the G- and D-peaks start to increase significantly. The Raman spectra become very broad after 500 h of milling but the change is a little thereafter up to 5000 h.

Figures 2(a) and (b) show the variation in the absolute intensity of the Raman spectra for the agate and the stainless ball-mills, respectively. An unusual increase of the absolute intensity is seen only for the agate ball-mill: the absolute Raman intensity of graphite powder gradually increases up to $\sim$100 h and then it remarkably increases, reaching a value of about 20 times larger than the original value after 1000 h of milling. The absolute intensity for the stainless ball-milled graphite, on the other hand, gradually decreases, exhibiting some fluctuation. These difference will be discussed in terms of the effect of impurities mixed during milling in Section IV.3.

To get further information on the changes of the two peak intensity ratio, the peakwidth and the peak position, the Raman spectra are deconvoluted with a least square algorithm. The spectra with a sharp feature, which correspond to graphite powders milled with the agate ball-mill at all the intervals and milled with the stainless ball-mill below 100 h, can be fitted with four Lorenzian peaks, consisting of two dominant Lorenzian peaks at about 1355 and 1580 $cm^{-1}$ and additional two minor Lorenzian peaks at about 1200 and 1500 $cm^{-1}$, as

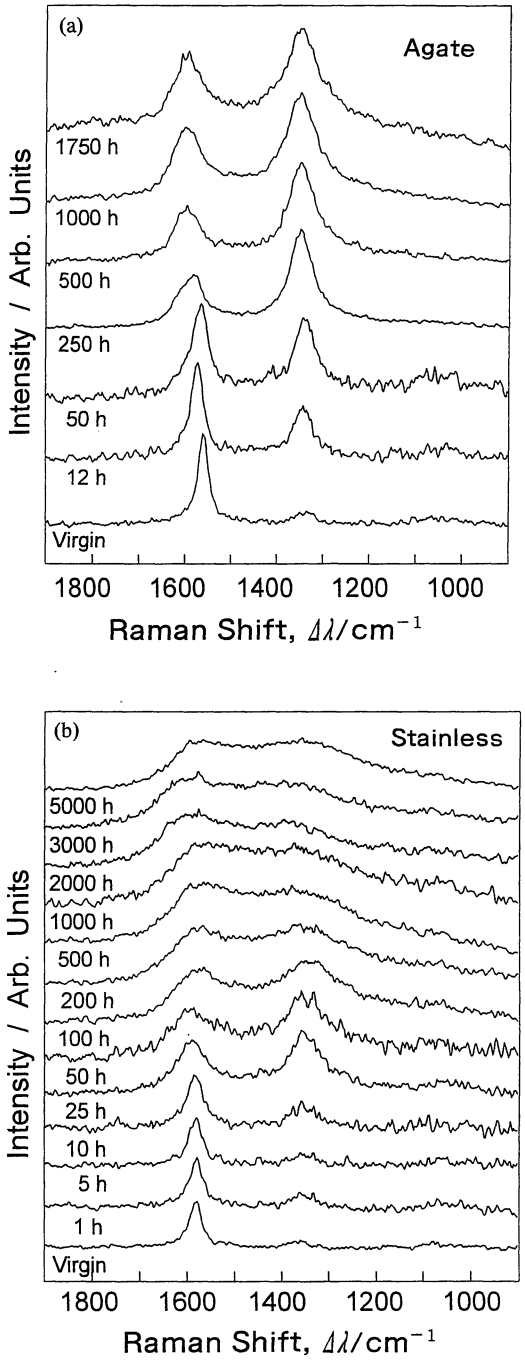


Fig. 1 Changes in Raman spectra of graphite mechanically milled with (a) agate ball-mill and (b) stainless ball-mill after different milling periods. A Raman spectrum of virgin graphite is shown at the bottom.

shown in Fig. 3 for example. While the broadened Raman spectra of graphite milled with the stainless ball-mill above 200 h cannot be fitted with Lorenzians anymore but could with four Gaussians as shown in Fig. 4(a). These broad spectra can be fitted also just with two dominant peaks at 1355 and 1580 $cm^{-1}$ as shown in Fig. 4(b), of which fitting has been given for amorphous carbon[12]. Since the change of Raman spectra is continuous from the initial graphite structure to the amorphous

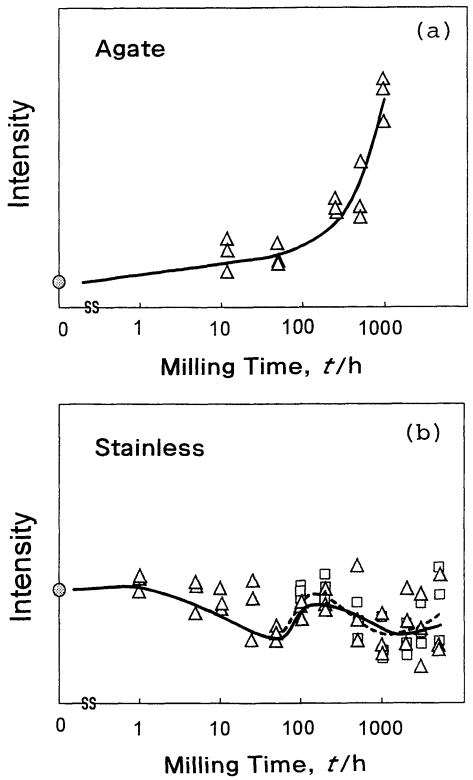


Fig. 2 Absolute intensity of Raman spectra of graphite mechanically milled with (a) agate ball-mill and (b) stainless ball-mill to different milling periods.

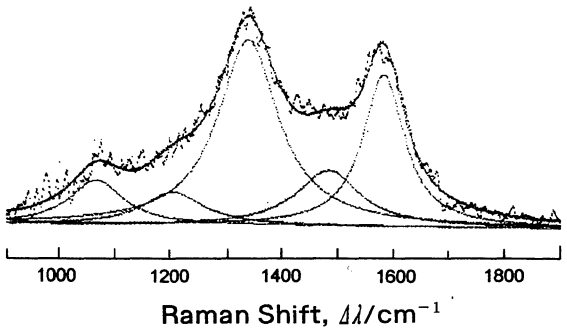


Fig. 3 A Raman spectrum fitted with four Lorenzian peaks, which are two dominant peaks at ~1355 and ~1580 $cm^{-1}$, and two minor peaks at ~1200 and ~1500 $cm^{-1}$. A small peak at ~1050 $cm^{-1}$ is a noise. Graphite is mechanically milled with stainless ball-mill to 50 h.

phase as seen in Fig. 1(b), we will discuss mainly with the results by the four peak fitting analysis, hereafter.

Figures 5(a) and (b) compare the intensity ratio ($I_{1355}/I_{1580}$) for the agate and the stainless ball-milled graphite as a function of logarithmic milling time, respectively. In-plane crystalline size La calculated by $I_{1355}/I_{1580}$ with Tuinstra and Koenig's empirical relation[13] is also indicated in the figures. For the agate ball-mill, the change can be roughly classified into three stages of A (0-~10 h), B (~10-~500 h), and C (~500-1750 h), as shown in Fig. 5(a). The $I_{1355}/I_{1580}$ gradually increases in Stage A and steeply increases in Stage B while it turns to decrease in Stage C. Similarly the change of $I_{1355}/I_{1580}$ for the stain-

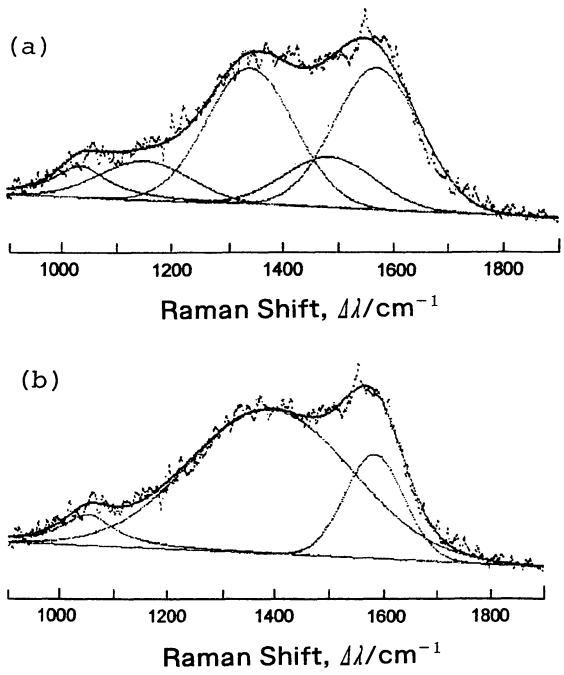


Fig. 4 Raman spectra fitted with (a) four Gaussian peaks, which are two dominant peaks at ~1355 and ~1580 $cm^{-1}$, and two minor peaks at ~1200 and ~1500 $cm^{-1}$ and (b) two Gaussian peaks at ~1355 and ~1580 $cm^{-1}$. A small peak at 1050 $cm^{-1}$ is a noise. Graphite is mechanically milled with stainless ball-mill to 1000 h.

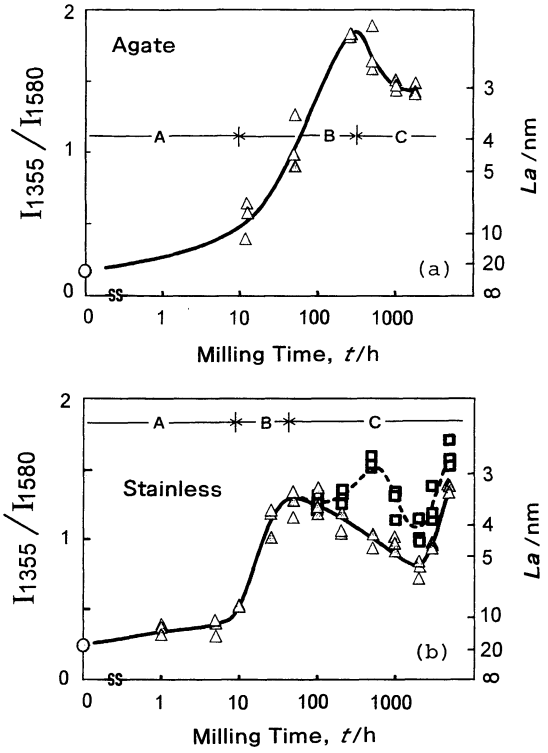


Fig. 5 Raman intensity ratio ($I_{1355}/I_{1580}$) of graphite mechanically milled with (a) agate ball-mill and (b) stainless ball-mill to different milling periods. The results with the four peak fitting and with the two peak fitting are indicated with solid and dotted curves, respectively.

less ball-milled graphite can be classified into the above three stages as shown in Fig. 5(b), but the start of Stage C is at ~50 h which is about 10 times earlier than that for the agate ball-mill. Furthermore, the minimum size of La calculated with the $I_{1355}/I_{1580}$ for the stainless ball-milled graphite is larger than that for the agate ball-milled graphite.

The peakwidth of the G-peak ($FWHM_{1580}$) also exhibits different behavior between the agate and the stainless ball-milled graphite as shown in Figs. 6(a) and (b), respectively. For the agate ball-mill the $FWHM_{1580}$ gently increases up to 1000 h and the change is a little among the three stages. For the stainless ball-mill, on the other hand, the $FWHM_{1580}$ gently increases to ~10 h and then steeply increases to 200 h, finally level off at about 160 $cm^{-1}$. We can clearly distinguish the change from Stage A to Stage B but the change between Stage B and Stage C is little on the results given by the four peak fitting method. Contrary to this, the two peak fitting can clearly distinguish the start of Stage C at ~500 h, as shown by a dotted curve.

Furthermore, the variation of the G-peak shift shows a characteristic difference between the agate and the stainless ball-milled graphite, as shown in Figs. 7(a) and (b), respectively. For the agate ball-mill, the G-peak at 1580 $cm^{-1}$ upshifts a little in Stage A and then it steeply increases in Stage B and Stage C, finally reaching 1615

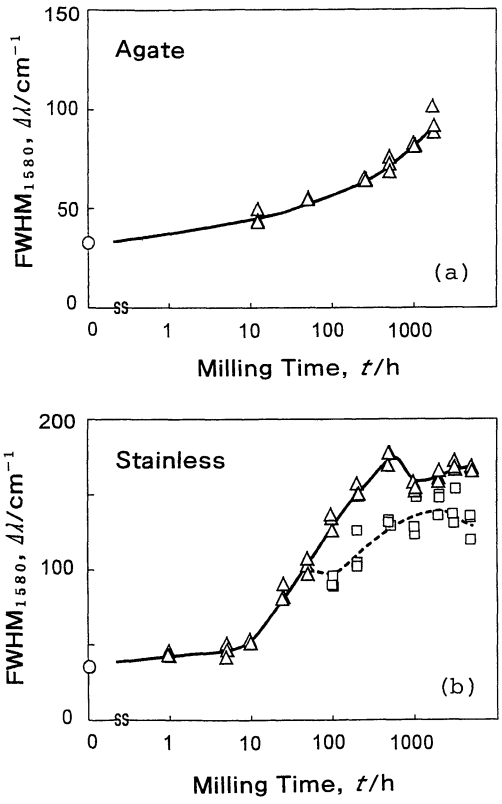


Fig. 6 Full width at half maximum of the G-peak ($FWHM_{1580}$) of graphite mechanically milled with (a) agate ball-mill and (b) stainless ball-mill after different milling periods. The results with the four peak fitting and with the two peak fitting are indicated with solid and dotted curves, respectively.

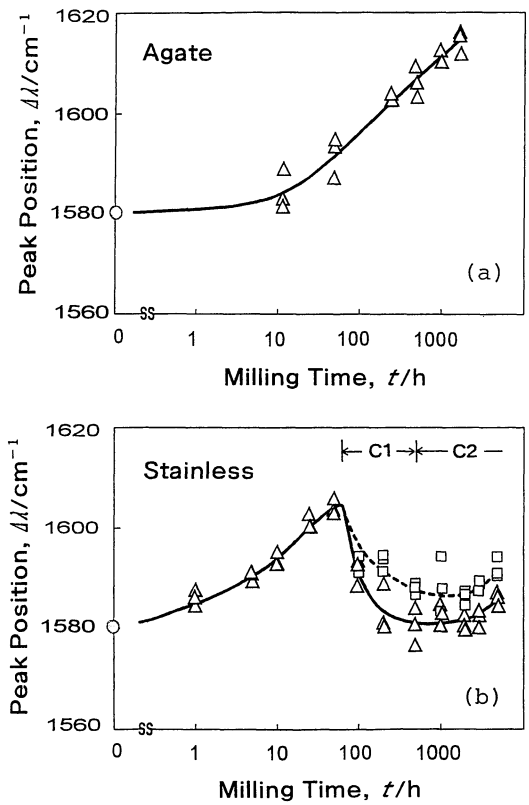


Fig. 7 Peak position of the G-peak of graphite mechanically milled with (a) agate ball-mill and (b) stainless ball-mill after different milling periods. The results with the four peak fitting and with the two peak fitting are indicated with solid and dotted curves, respectively.

$cm^{-1}$ at 1950 h. It is difficult to find the change between Stage B and Stage C. For the stainless ball-mill, on the other hands, the G-peak gradually upshifts in Stage A and the upshift rate increases a little in Stage B, reaching 1605 $cm^{-1}$ at ~50 h. After that, the G-peak turns to downshift and levels off at ~500 h. From the changes in the $I_{1355}/I_{1580}$, the $FWHM_{1580}$ and the peak position, Stage C for the stainless ball-milled graphite can be roughly classified into two stages of C1 (~50–500 h) and C2 (~500–5000 h), as shown in Fig. 7(b).

Graphite milled with the agate ball-mill to 250 and 1750 h are annealed up to 873 K. Both of the Raman spectra scarcely change as shown in Figs. 8(a) and (b), thereby exhibiting rather thermally stable structure after the milling.

### Diamond milled with a stainless ball-mill

Figure 9 shows the variation in Raman spectra of diamond during a stainless ball-milling. The absolute intensity of the diamond peak at 1332 $cm^{-1}$ is seen to decrease to about 1/10 of the virgin diamond at 100 h, finally disappearing at 450 h. We can not detect a broad spectrum, which is found for the stainless ball-milled graphite above 500 h of milling.

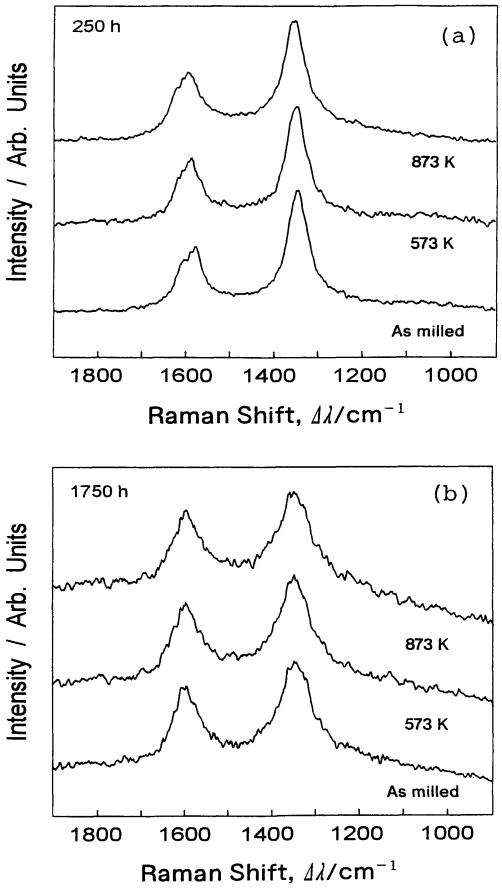


Fig. 8 Changes in Raman spectra on annealing at 573 and 873 K for 30 min for graphite mechanically milled with agate ball-mill to (a) 250 h and (b) 1750 h.

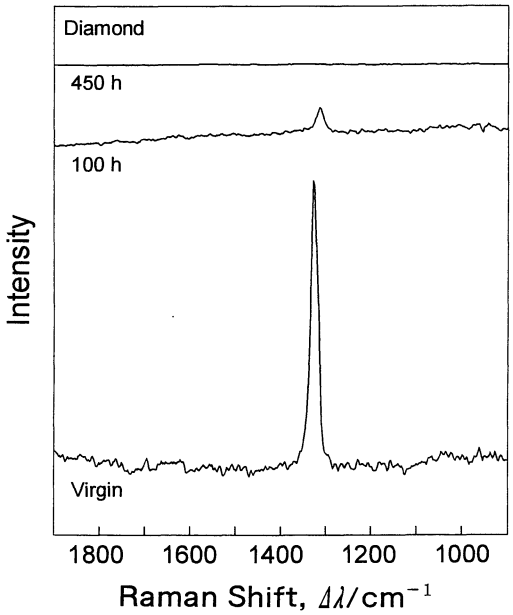


Fig. 9 Raman spectra of diamond mechanically milled with stainless ball-mill to 100 and 450 h. The Raman intensity is expressed in the absolute value.

## IV. Discussion

### 1. Amorphization of graphite by ball-milling

The results of the Raman spectra analyzed by a least square fitting clearly show a difference between the agate and the stainless ball-milled graphite. A most clear difference is the downshift of the G-peak position, which is seen only for the stainless ball-milled graphite in Stage C ($> \sim 50$ h). Correspondingly, the Raman spectra of the stainless ball-milled graphite significantly change in the shape. The Raman spectra, which can be fitted by Lorenzian below $\sim 50$ h, cannot be fitted by Lorenzian anymore after $\sim 200$ h but by Gaussian with four or two peaks. The Raman spectra of the agate ball-milled graphite, on the other hand, can be fitted with four Lorenzian peaks for all the milling times up to 1750 h. Such a significant downshift of the G-peak position and the change of Raman spectral shape from Lorenzian to Gaussian have been found also for ion irradiated graphite and explained by C-A transition[7]. In addition to the downshift of the G-peak, a decrease of the $I_{1355}/I_{1580}$ and an increase of the $FWHM_{1580}$ to a very large value of $\sim 190\ cm^{-1}$ have been found for the amorphizing graphite under irradiation, which are also found for the stainless ball-milled graphite.

From these correspondence on the change of the Raman spectra between the stainless ball-milled graphite and the ion irradiated graphite, it is suggested that the onset and the completion of amorphization for the stainless ball-milled graphite correspond to the onsets of Stage C1 ($\sim 50$ h) and Stage C2 ($\sim 500$ h), respectively. X-ray diffraction measurement has also confirmed the completion of amorphization at the onset of Stage C2 by the disappearance of sharp graphite peak[14], However, one should note the final value of the $FWHM_{1580}$, which is $\sim 170\ cm^{-1}$ in Stage C2, is less than that of irradiation-induced amorphized graphite of $\sim 190\ cm^{-1}$. This implies that the amorphized graphite by milling is less disorder in the structure compared to the one produced by ion irradiated graphite.

For the agate ball-milled graphite, on the other hand, one cannot find the downshift of the G-peak in Stage C though the $I_{1355}/I_{1580}$ turns to decrease. As the $FWHM_{1580}$ is still increasing in Stage C, the reduction of $I_{1355}/I_{1580}$ should not be attributed to the increase of the crystalline size La, i.e. recrystallization, during milling, but to an increase of some disorder. Then, Stage C for the agate ball-milled graphite may correspond to an introduction of partial disorder.

### 2. Reduction of crystalline size and chemical effect of impurity

According to Tuinstra and Koenig[13], the intensity ratio of $I_{1355}/I_{1580}$ has been shown to be inversely proportional to the in-plane crystalline size La of various grades of graphite investigated by X-ray diffraction. Recently, Niwase *et al.* have shown a significant decrease of the $I_{1355}/I_{1580}$ of $D^+$ irradiated highly oriented pyrolytic graphite (HOPG) on annealing at 473 K where vacancy is

immobile. From the result they concluded that the formation of Frenkel pairs can originate in the increase of the $I_{1355}/I_{1580}$[15]. As shown in Fig. 8, however, the $I_{1355}/I_{1580}$ which increased by the ball-milling did not decrease on anneallng up to 873 K. This suggests that the milling process does not produce Frenkel pairs. Then, the increase of the $I_{1355}/I_{1580}$ is considered to correspond to the reduction of the crystalline size La.

The change in the $1/La$ before amorphization can be classified by Stage A and Stage B against the logarithmic milling time both for the agate and the stainless ball-milled graphite as shown in Figs. 5(a) and (b). Taking account of the anisotropy of graphite structure, one can guess that the two stages probably correspond to the reductions of the crystalline size Lc along the c-axis and La in the basal plane: i.e. in Stage A milling energy is considered to be mainly used on the cleavage between the basal planes and then not used so much to the reduction of La. While in Stage B most of the milling energy can be given to the reduction of La, thereby leading to the higher reduction rate of La than in Stage A. Nevertheless, further direct investigation on the morphological change during milling is awaited on the confirmation.

One should note that the ultimate crystalline size La of 2.5 nm estimated by the $I_{1355}/I_{1580}$ for the agate ball-milled graphite is less than that of 3.5 nm for the stainless ball-milled graphite. Moreover, the milling time to reach the ultimate crystalline size for the former is about 10 times larger than that for the latter. These results indicate that the nanocrystalline graphite produced by the stainless ball-mill is much more unstable than that formed by the agate ball-mill and, therefore, C-A transform occurs earlier with larger size. Also it should be noted that the increase rate of the $FWHM_{1580}$ against the $I_{1355}/I_{1580}$, which may indicate the amount of disorder[11], for the stainless ball-mill (Fig. 6(b)) is higher than that for the agate ball-mill (Fig. 6(a)): the $FWHM_{1580}$ reaches a value of 130 $cm^{-1}$ when the $I_{1355}/I_{1580}$ reaches a value of 1 for the former and this value is larger than 50 $cm^{-1}$ for the latter for example. This indicates that some disordered structure is continuously introduced during the stainless ball-milling in addition to the reduction of the crystalline size La.

Tanaka *et al.* have investigated the mechanical alloying of iron and graphite powders in composition range $Fe_{1-x}C_x$ ($x=0.17$–$0.90$) and showed that the graphite peaks in X-ray diffraction disappear at 200 h for all the composition range[16][17]. This indicates that graphite easily amorphizes during milling when Fe atoms coexist. Meanwhile, mixing of Fe atoms during stainless ball-milling has been pointed out by some authors[3][4]. Therefore, the earlier amorphization at larger crystalline size for the stainless ball-milled graphite found in the present study is probably originate in the impurity effect of Fe mixed during milling. As the basal plane of graphite is chemically inert and point defects are not formed during the milling, the chemical reaction between iron and carbon atoms are considered to occur at the boundary of graphite particle, i.e. the edge of the basal plane of graphite. This implies that the amorphization of the nanocrystalline graphite milled with the stainless ball mill is mainly controlled by the chemical state of the grain boundary.

Similar consideration can be given for the amorphization of diamond induced by the stainless ball-milling. It is shown that diamond does not amorphize under electron irradiation[8] but by ion irradiation[9][10]. These results suggest that diamond is more stable than graphite against the cutting of the bonding, i.e. it is difficult to amorphize diamond only by reduction of crystalline size. However, as shown in the present results, the milling time for amorphization with a stainless ball-mill is more less than that for the agate ball-milled graphite. Therefore, the amorphization of diamond is considered to be also enhanced by chemical reaction with Fe atoms at the nanocrystalline boundary.

One should note that the ultimate crystalline size of 2.5 nm of graphite produced by the agate ball-mill is the smallest size of nanocrystalline materials, which have ever been made. Moreover, this is probably the smallest size of artificial graphite without significant disorder. Then, it may be an interesting topic to check its potential as a new material.

### 3. Enhanced Raman intensity for the agate ball-milled graphite

One of significant differences in the change of Raman spectra between graphite powders milled with the agate and the stainless ball-mills is the unusual increase of the Raman intensity only detected for the agate ball-mill. We can mention two possibilities on the enhancement of Raman intensity; one is the increase of the surface area due to the crystalline size reduction and the other is the effect of agate particles mixed during the ball-milling, of which existence may enhance the Raman intensity. One should note that the enhancement occurs in Stage C significantly, which does not correspond to the reduction of crystalline size. Moreover, marked increase of $SiO_2$ which is main element of agate is detected by X-ray diffraction in Stage C[14]. These results strongly suggest that the unusual increase of the Raman intensity may be induced by some cooperative effect between $SiO_2$ and nanocrystalline graphite. However, there is no report on the surface enhanced Raman scattering by $SiO_2$ though there are so many reports by several kinds of metal or metal oxides[18], Therefore, further investigation is needed to clarify the origin of the unusual intensity increase.

## V. Conclusions

Pure elements of graphite and diamond are mechanically milled with agate or stainless ball-mills and their structural changes are investigated by Raman spectroscopy. The results obtained are summarized as follows:

(1) An unusual enhancement of the Raman intensity of graphite during milling is only found for the agate ball-mill.

(2) The Raman spectra analyzed with a least square fitting showed three characteristic stages on the change of the $I_{1355}/I_{1580}$, which probably correspond to the cleavage

between the basal planes, the reduction of the crystalline size of the basal plane, and the amorphization, respectively.

(3) The ultimate crystalline size of graphite, estimated by the Raman intensity ratio ($I_{1355}/I_{1580}$), of 2.5 nm for the agate ball-mill is smaller than that of 3.5 nm for the stainless ball-mill, while the milling time to reach the ultimate size for the former is about 10 times larger than that for the latter, indicating more stability of the nanocrystalline graphite.

(4) A significant broadening of the Raman spectra, which indicates the completion of amorphization, is detected only for the stainless ball-milled graphite. Also the increase rate of the Raman peakwidth for the stainless ball-milled graphite before amorphization is higher than that for the agate ball-milled graphite, indicating a larger introduction of disorder from the beginning of milling. The instability of nanocrystalline graphite produced by the stainless ball-mill is explained by some chemical effect of Fe, which mixed during milling from the apparatus.

(5) Amorphization of diamond is also observed for the stainless ball-mill. However, a broad Raman spectra which observed for the amorphized graphite is not detected.

*Acknowledgments*

Raman measurements were performed at the Institute of Scientific and Industrial Research of Osaka University. The authors would like to express their thanks to Prof. T. Tanabe, Prof. Y. Miyamoto and Dr. I. Tanaka for valuable discussions.

REFERENCES

(1) E. Hellstern, H. J. Fecht, Z. Fu, and W. L. Johnson: J. Appl. Phys., **65** (1989), 305.
(2) H. J. Fecht, E. Hellstern, Z. Fu, and W. L. Johnson: Metall. Trans. A, **21A** (1990), 2333.
(3) J. Echert, J. C. Holzer, C. E. Krill III and W. L. Johnson: Mater. Science Forum, **88–90** (1992), 505.
(4) E. Gaffet and M. Harmelin: J. Less-common Metals, **157** (1990), 201.
(5) O. W. Holland and S. J. Pennycook: Appl. Phys. Lett., **55** (1989), 2503.
(6) K. Nakai, C. Kinoshita and A. Matsunaga: Ultramicroscopy, **39** (1991), 361.
(7) K. Niwase and T. Tanabe: Mater. Trans., JIM, **34** (1993), 1111.
(8) J. Koike, T. E. Mitchell and D. M. Parkin: Appl. Phys. Lett., **59** (1991), 2515.
(9) M. S. Dresselhaus and R. Kalish: *Ion Implantation in Diamond, Graphite and Related Materials*, Springer-Verlag, (1992), p. 129.
(10) K. Niwase, Y. Kakimoto I. Tanaka and T. Tanabe: Nucl. Instr. Meth., **B91** (1994), 78.
(11) K. Niwase: Phys. Rev., B, in press.
(12) M. Yoshikawa, G. Katagiri, H. Ishida and A. Ishitani: Solid. State Commun., **66** (1988), 1177.
(13) F. Tuinstra and J. L. Koenig: J. Chem. Phys., **53** (1979), 1126.
(14) T. Tanaka *et al.*: to be published.
(15) K. Niwase, T. Tanabe and I. Tanaka: J. Nucl. Mater., **191–194** (1992), 335.
(16) T. Tanaka, S. Nasu, K. N. Ishihara and P. H. Shingu: J. Less-Common Metals, **171** (1991), 237.
(17) T. Tanaka, S. Nasu, K. Nakagawa, K. N. Ishihara and P. H. Shingu: Mater. Science Forum, **88–90** (1992), 269.
(18) M. Moskovits: Rev. Mod. Phys., **57** (1985) 783.